PHILOSOPHICAL TRANSACTIONS OF THE ROYAL SOCIETY A

Phil. Trans. R. Soc. A (2009) **367**, 3379–3400
doi:10.1098/rsta.2009.0088

Continuum model of epithelial morphogenesis during *Caenorhabditis elegans* embryonic elongation

By P. Ciarletta[1], M. Ben Amar[1,*] and M. Labouesse[2]

[1]*Laboratoire de Physique Statistique, École Normale Supérieure, 24 rue Lhomond, 75231 Paris Cedex 05, France*
[2]*Institut de Génétique et de Biologie Moléculaire et Cellulaire, CNRS/INSERM/ULP, 1 rue Laurent Fries, BP 10142, 67404 Illkirch Cedex, France*

The purpose of this work is to provide a biomechanical model to investigate the interplay between cellular structures and the mechanical force distribution during the elongation process of *Caenorhabditis elegans* embryos. Epithelial morphogenesis drives the elongation process of an ovoid embryo to become a worm-shaped embryo about four times longer and three times thinner. The overall anatomy of the embryo is modelled in the continuum mechanics framework from the structural organization of the subcellular filaments within epithelial cells. The constitutive relationships consider embryonic cells as homogeneous materials with an active behaviour, determined by the non-muscle myosin II molecular motor, and a passive viscoelastic response, related to the directional properties of the filament network inside cells. The axisymmetric elastic solution at equilibrium is derived by means of the incompressibility conditions, the continuity conditions for the overall embryo deformation and the balance principles for the embryonic cells. A particular analytical solution is proposed from a simplified geometry, demonstrating the mechanical role of the microtubule network within epithelial cells in redistributing the stress from a differential contraction of circumferentially oriented actin filaments. The theoretical predictions of the biomechanical model are discussed within the biological scenario proposed through genetic analysis and pharmacological experiments.

Keywords: morphogenesis; *Caenorhabditis elegans*; embryo elongation; mechanobiology; biomechanics

1. Introduction

Caenorhabditis elegans (*C. elegans*) is a free-living nematode (a roundworm), which is heavily used as a biological model because of its simplicity, rapid growth rate (3.5 days from fecundation to adult form) and its transparency.[1] Elongation of the *C. elegans* embryo is the biological process during which an

*Author for correspondence (benamar@lps.ens.fr).

[1]For further details, readers are referred to the following databases: www.wormatlas.org (for anatomy), www.wormbase.org (for genetic and genomic data) and www.wormbook.org (for biology).

One contribution of 12 to a Theme Issue 'Mechanics in biology: cells and tissues'.

ovoid embryo with 556 cells becomes a worm-shaped embryo about four times longer, from 60 to 250 μm long, and three times thinner (Chisholm & Hardin 2005). This process, which lasts approximately 2 h, does not involve any cell division, nor any change in cell position. It is driven by cell shape changes of epidermal cells and the underlying muscles.

The purpose of this work is to model the epithelial morphogenesis during *C. elegans* embryonic elongation, investigating the structural role of the subcellular filaments during the process. The biomechanical problem is defined using the fundamental assumption that the embryo may be considered as having a piecewise continuous distribution of matter in space and time. This hypothesis implies that the embryonic cells can be considered as an assembly of continuum bodies, i.e. made of a continuous set of material points having macroscopic dimensions that are much larger than intercellular spacings (Lim *et al.* 2006). The mechanical properties of the cell are largely determined by the cytoskeleton (Kasza *et al.* 2007). The continuum approach considers the embryonic cells as biopolymeric networks of *their* three major structural filaments: F-actin, intermediate filaments (IFs) and microtubules (MTs). Two important parameters for determining the mechanical contribution of biological filaments inside the cell are the so-called *persistence length* l_{p}, defined as the typical length for the decay of tangent–tangent correlations, and the *contour length* l_{c}. Polymer theories consider a filament rigid when $l_{\mathrm{c}} \ll l_{\mathrm{p}}$ and flexible (or purely entropic elastic) when $l_{\mathrm{p}} \ll l_{\mathrm{c}}$ (Boal 2002). Cellular filaments belong to the intermediate category of semiflexible filaments, having comparable values of l_{p} and l_{c}, and their mechanical behaviour is determined by their network organization and cross-links (Storm *et al.* 2005). IFs have values of persistence length l_{p} in the range of 300 nm to slightly over 1 μm, with a Young's modulus of about 300–400 MPa. Gels of IFs result in a compliant elastic behaviour, but they are capable of withstanding very large deformations before breaking (up to 300%), owing to IFs' unique structure of overlapping α-helical coiled-coil subunits (Wagner *et al.* 2007). F-Actin has a filamentous structure with a diameter of 7 nm, values of persistence length of about 3–17 μm and contour length from 0.1 μm (*in vivo*) up to 20 μm (*in vitro*), with a typical Young's modulus of about 1–2 GPa (Chauduri *et al.* 2007). The rheology of cross-linked F-actin networks has been extensively investigated (Janmey *et al.* 1994), demonstrating that the stiffening contribution of the filaments in tension is sufficiently strong to stabilize the cells. MTs are composed of several tubulin protofilaments assembled with helical symmetry to form hollow cylindrical tubes, with an inner and an outer diameter of about 15 and 25 nm, respectively. Such a structure gives MTs a bending rigidity that is 100 times greater than that of IFs and F-actin, allowing them to accomplish multiple tasks in the cell. The persistence length of MTs has been reported to be 1–6 mm, being tens of times longer than the typical size of a cell, with a Young's modulus ranging from 0.1 to 7 GPa (Pampaloni & Florin 2008). Although highly resistant to thermal fluctuations, MTs inside cells have been visualized with localized bends of only a few micrometres, suggesting that they experience compressive non-thermal loads (i.e. arising from myosin contractility or from polymerization) that induce short-wavelength buckling phenomena (Brangwynne *et al.* 2006). Therefore, MTs are at once very stiff biopolymers if subjected to pulling forces and highly resilient structures in order to resist strong contractile forces.

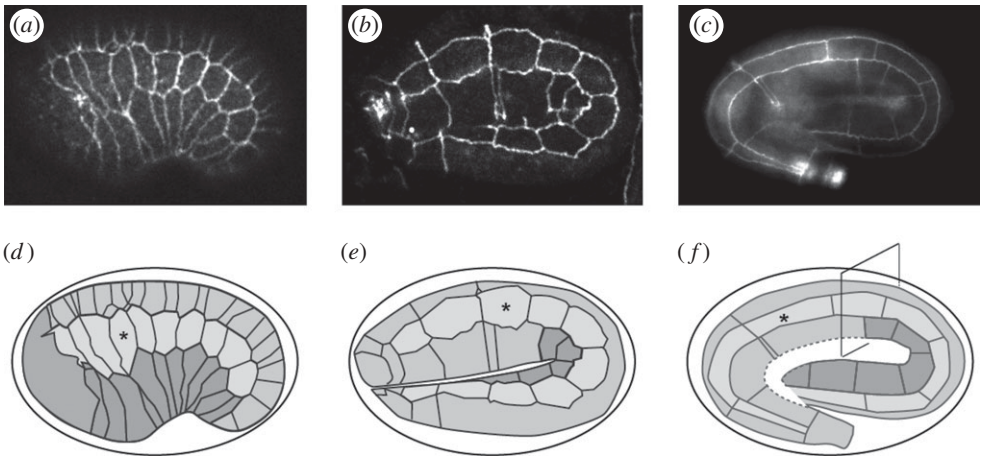

Figure 1. Cellular anatomy of the elongating *C. elegans* embryo. (*a–c*) Lateral views of *C. elegans* embryos at three different stages, as visualized with an antibody against the junctional component AJM-1 (Koppen *et al.* 2001): (*a*) beginning of elongation (the so-called lima bean stage); (*b*) after the formation of syncytia when muscles start to contract (the so-called twofold stage); and (*c*) late elongation (the so-called pretzel stage with the posterior part of the body out of focus). The eggshell is approximately $50 \times 20\,\mu m$; anterior is to the left, dorsal is up. (*d–f*) Camera lucida drawings of the images shown in (*a–c*) with grey shades indicating the major epidermal cell types. Star, same cell at different stages.

In the following, the structure of the *C. elegans* embryo and the subcellular anatomy of its constituent cell families are discussed in §2. The kinematic and constitutive description of the embryonic elongation process in the continuum framework is derived in §3, accounting for the active and passive responses of the biological networks. The axisymmetric solution at thermodynamic equilibrium is presented in §4, discussing the role of cellular filaments in the distribution of forces during the elongation process. Finally, §5 discusses the results of the biomechanical model, with a particular focus on the theoretical guidelines for future experiments.

2. Structure and subcellular anatomy of the *Caenorhabditis elegans* embryo

The embryo is composed of an outer epidermal layer, an inner digestive tube running from head to anus in the tail, four rows of muscles located between the epidermis and the digestive tract, and many neurons that are mostly located in the head and account for the larger head diameter. The cellular anatomy of the elongating *C. elegans* embryo is depicted in figure 1. During the first part of elongation, the embryo is slightly conical, as its head has a larger section compared with its tail. During the second part, its section is more regular from head to tail, except at the termini. The epidermis surrounding the *C. elegans* embryo is initially organized into six rows of cells, with approximately 12 cells per row. Early during the elongation process, many cells fuse to generate several syncytia: the largest one includes 17 dorsal cells and 4 ventral cells, which cover the dorsal

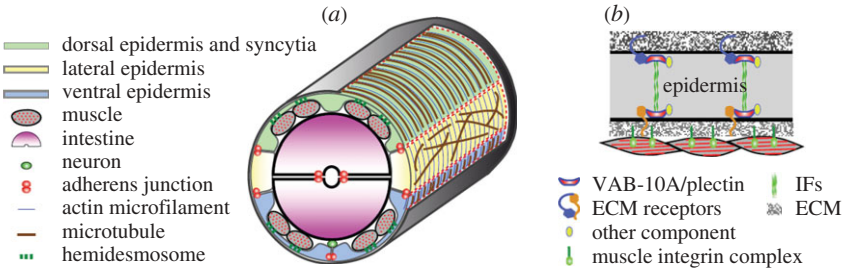

Figure 2. (*a*) Cross section through the body showing the internal anatomy at the level of the 'window' in figure 1*f*. The outer ECM and apical plasma membrane have been removed over part of the embryo to reveal the organization of the actin microfilaments and MTs. Microfilaments form thicker bundles in the dorsal and ventral epidermis. MTs are circumferentially oriented only in the dorsal and ventral epidermis, where they are overall interspersed with microfilaments. (*b*) Structure of the muscle–ECM–epidermis–ECM attachment featuring two inverted hemidesmosome-like junctions in the epidermis bridged by IFs.

posterior two-thirds of the embryo; the other syncytia are located in the head and are smaller (for details, see http://www.wormatlas.org/handbook/hypodermis/hypodermis.htm). Lateral cells (also called seam cells) and the central ventral cells do not fuse. The presence of large syncytia must have a very significant influence on the distribution of forces in the embryo. Muscle cells, which are anchored to the ventral and dorsal epidermis through specific structures, do not fuse, although their ultrastructure and organization resemble that of vertebrate muscles.

Epidermal cells are held together through adherens junctions located subapically. *C. elegans* adherens junctions display all the features of classical adherens junctions; in particular, they include E-cadherin, β-catenin and α-catenin homologues that anchor an actin belt (Labouesse 2006). In addition, each epidermal cell harbours an array of circumferentially oriented parallel and evenly spaced actin microfilament bundles that are attached to adherens junctions. These microfilaments are initially very short, quite dynamic and become organized in parallel bundles during the first half of elongation (Priess & Hirsh 1986), which after mid-elongation appear to run from one junction to the next; the precise organization of actin microfilaments within these bundles is not known and might be different in different cells. There are also circumferentially oriented parallel MTs in dorsal and ventral cells, although there seems to be no direct connection between MTs and junctions. In contrast, MTs in lateral cells are not circumferentially oriented until the end of elongation and form a circular network parallel to all junctions (Priess & Hirsh 1986).

A cross section of the embryo, showing its internal anatomy and the mechanisms of muscle attachments, is shown in figure 2. Muscle cells are anchored to the extracellular matrix (ECM) separating them from the basal plasma membrane of the dorsal and ventral epidermis (Labouesse 2006). At those positions, the epidermis assembles two inverted hemidesmosome-like junctional complexes facing each other, one at the basal surface in contact with muscle ECM and the other at the apical surface in contact with the outer ECM. The hemidesmosome-like junctions include a plectin/BPAG-1e homologue (called VAB-10A) and IFs, like in vertebrates (Bosher *et al.* 2003; Woo *et al.* 2004);

however, ECM receptors are distinct from integrins. The outer ECM corresponds to a molecularly ill-defined embryonic shield during elongation and the cuticle afterwards. The epidermis is very thin at the level of hemidesmosomes (typically 50–100 nm thick), such that muscles are effectively anchored to the cuticle and can transmit their contractions to the body to generate movement. In the following, a biomechanical model in nonlinear elasticity is built in accordance with the structural organization of the subcellular filaments within the epithelial cells and with the overall anatomy of the *C. elegans* embryo.

3. Biomechanical model of the embryonic elongation

(*a*) *Geometry of the embryo and kinematic description*

Let Ω_0 be the fixed reference configuration of the embryo in the not-elongated state at $t=0$. The geometry of the epidermis of the *C. elegans* embryo is described in the reference configuration by a simplified model composed of:

(i) a truncated spherical head having an internal radius R_h, an opening angle $\phi_\mathrm{h}=\pi/2+\alpha$ and thickness H_h;
(ii) a truncated cone body of circular section (made of the dorsal, the lateral and the ventral cells referred to by the subscripts d, l and v in the following, respectively) having a head internal radius $R_0=R_\mathrm{h}\cos\alpha$, a total length L and a tail internal radius $R_1=R_0-L\tan\alpha$. Every cell family is modelled having constant values of thickness H^i and angular extension $\Delta\Theta^i$ ($i=\mathrm{d},\mathrm{l},\mathrm{v}$). We may define Θ^i_in and Θ^i_fin as the initial and final angular coordinates for each cell family in the undeformed configuration, so that $\sum_i\Delta\Theta^i=\sum_i(\Theta^i_\mathrm{fin}-\Theta^i_\mathrm{in})=2\pi$; and
(iii) a truncated spherical tail having an internal radius $R_\mathrm{t}=R_1\cos\alpha$, an opening angle $\phi_\mathrm{t}=\pi/2-\alpha$, and thickness H_t.

The biological matter inside the embryonic shell is supposed to be homogeneous, and it is referred to with the superscript m in the following.

The description of the deformation can be defined by a mapping $\chi\colon \Omega_0\to\Re^3$ that transforms the material point $\mathbf{X}\in\Omega_0$ to a position $\mathbf{x}=\chi(\mathbf{X},t)$ in the deformed configuration Ω.

The deformation tensor $\mathbf{F}$ is defined as (Fung 1981)

$$\mathbf{F}=\frac{\partial\chi(\mathbf{X},t)}{\partial\mathbf{X}}=\mathrm{Grad}\,\mathbf{x}(\mathbf{X},t), \tag{3.1}$$

where Grad indicates the gradient in material coordinates.

The material time derivative $\dot{\mathbf{F}}$ of the deformation tensor $\mathbf{F}$ is defined as

$$\dot{\mathbf{F}}=\frac{\partial}{\partial t}\frac{\partial\chi(\mathbf{X},t)}{\partial\mathbf{X}}=\frac{\partial}{\partial\mathbf{X}}\frac{\partial\chi(\mathbf{X},t)}{\partial t}=\frac{\partial\mathbf{V}(\mathbf{X},t)}{\partial\mathbf{X}}=\mathrm{Grad}\,\mathbf{V}(\mathbf{X},t) \tag{3.2}$$

and gives the time rate of change of the deformation, the material velocity gradient being Grad $\mathbf{V}$.

Most constitutive relations in finite elasticity associate the state of deformation with components of the right and the left Cauchy tensors, defined as $\mathbf{C}=\mathbf{F}^\mathrm{T}\mathbf{F}$ and $\mathbf{b}=\mathbf{F}\mathbf{F}^\mathrm{T}$, respectively. Considering a generic unit vector $\mathbf{a}_0$ in the reference

configuration that is deformed to a vector **a** in the current configuration, the length λ_a of the deformed vector **a** can be expressed as

$$\lambda_a^2 = \mathbf{a_0} \cdot \mathbf{C}\mathbf{a_0} \quad \text{and} \quad \lambda_a^{-2} = \mathbf{a} \cdot \mathbf{b}^{-1}\mathbf{a}. \tag{3.3}$$

The (right) **C** and (left) **b** Cauchy deformation tensors express a fundamental strain measure in terms of material and spatial coordinates, respectively.

The change between the infinitesimal volumes $\mathrm{d}V$ and $\mathrm{d}v$, measured in the reference and deformed configuration, respectively, is given by

$$\frac{\mathrm{d}v}{\mathrm{d}V} = \det \mathbf{F} = J(\mathbf{X}, t) > 0, \tag{3.4}$$

where J is the determinant of the deformation gradient **F**, being positive to respect the principle of impenetrability of matter. Being composed primarily of water, the embryonic cells are assumed to behave as nearly incompressible materials (Caille *et al.* 2002), so that $\det \mathbf{F} = 1$.

(*b*) *Constitutive relationships for the active and passive responses of the embryo*

The determination of the material response of the elongating embryo requires knowledge of the mechanical response of continuum body undergoing finite deformations. Together with kinematic, stress and equilibrium equations, the constitutive equations for the materials are necessary to describe the state of stress and deformation inside the body. In the following, we will use the assumption that cells are made of homogeneous material, using constitutive laws that are not dependent on the position of the material point.

The expression of the free energy of the generic cellular aggregate i ($i = \mathrm{d}, \mathrm{l}, \mathrm{v}$) can be decoupled into the sum of a chemical contribution ψ^i_{ch}, due to the fluxes of monomers and motor molecules that generate active forces, and a mechanical contribution ψ^i_{mech}, due to the passive response of the material.

The non-muscle myosin II is the main molecular motor involved in epithelial morphogenesis during *C. elegans* embryonic elongation (Ding *et al.* 2004). Even if MTs are highly dynamic structures undergoing polymerization and depolymerization phases on the time scale of seconds (Desai & Mitchison 1997), and their dynamic activity in other biological processes seems to be related to the transport of key regulators of the activation of the actin–myosin II complex (Dawes-Hoang *et al.* 2005), they will be considered as passive filaments in the following. The non-muscle myosin II is an actin-based molecular motor: myosin II molecules, when bound to the antiparallel actin filaments attached to adherens junctions, consume adenosine triphosphate (ATP) and cause the motion of actin filaments, sliding past each other (Quintin *et al.* 2008). From a phenomenological point of view, the chemical free energy ψ^i_{ch} can be expressed as a function of the chemical potential difference $\Delta\mu^i$ between ATP and its hydrolysis products, adenosine diphosphate plus an inorganic phosphate, and the polarization field **p** of the actin filaments, defined for each filament as the average of the unit vectors pointing to one end in a small volume around each point (Callan-Jones *et al.* 2008). From the constitutive equation of active polar gels, whose extensive derivation has been proposed by Kruse *et al.* (2005), the active Cauchy stress

$\boldsymbol{\sigma}^i_{\mathrm{act}}(\Delta\mu^i, \mathbf{p})$ generated by the circumferential actin bundle in the embryo epithelial cell can be expressed as

$$\boldsymbol{\sigma}^i_{\mathrm{act}}(\Delta\mu^i, \mathbf{p}) = -\zeta\,\Delta\mu^i \cdot \mathbf{e}_\theta \otimes \mathbf{e}_\theta, \tag{3.5}$$

where $\mathbf{p} = \mathbf{e}_\theta$, the unit vector in the circumferential direction, and ζ is a material coefficient of the cytoskeleton characterizing the actin–myosin activity, being negative for contractile molecular motors.

Let us consider the epithelial cells as viscoelastic materials having an internal structure with a number m of dissipative phenomena that can be associated with internal tensor variables $\boldsymbol{\Gamma}_\alpha$, $\alpha = 1, \ldots, m$.

Considering an isothermal process, the free energy function ψ^i_{mech} related to the passive mechanical behaviour of the generic cell family i, considered per unit of reference volume, can be expressed as (Holzapfel & Simo 1996)

$$\psi^i_{\mathrm{mech}}(\mathbf{C}, \boldsymbol{\Gamma}_1, \ldots, \boldsymbol{\Gamma}_m) = \psi^i_{\mathrm{eq}}(\mathbf{C}) + \sum_{\alpha=1}^{m} \Upsilon_\alpha(\mathbf{C}, \boldsymbol{\Gamma}_\alpha), \tag{3.6}$$

where ψ^i_{mech} is the strain energy function related to the equilibrium state of the material and $\Upsilon_\alpha(\mathbf{C}, \boldsymbol{\Gamma}_\alpha)$ are dissipative potentials (or configurational free energies) related to the influence of the viscous processes in the non-equilibrium state. The stress-free configuration is identified by putting $\psi^i_{\mathrm{mech}}(\mathbf{I}) = \sum_{\alpha=1}^{m} \Upsilon_\alpha(\mathbf{I}, \mathbf{I}) = 0$.

A constitutive law for the passive response of the material, in terms of the Cauchy stress tensor $\boldsymbol{\sigma}^i_{\mathrm{pass}}$, can be expressed as

$$\begin{aligned}\boldsymbol{\sigma}^i_{\mathrm{pass}}(\mathbf{C}, \boldsymbol{\Gamma}_1, \ldots, \boldsymbol{\Gamma}_m) &= \boldsymbol{\sigma}^i_{\mathrm{eq}}(\mathbf{C}) + \sum_{\alpha=1}^{m} \boldsymbol{\sigma}^i_\alpha(\mathbf{C}, \boldsymbol{\Gamma}_1, \ldots, \boldsymbol{\Gamma}_m) \\ &= \frac{2}{\det \mathbf{F}} \left[\mathbf{F} \frac{\partial \psi^i_{\mathrm{eq}}(\mathbf{C})}{\partial \mathbf{C}} \mathbf{F}^{\mathrm{T}} + \sum_{\alpha=1}^{m} \mathbf{F} \frac{\partial \Upsilon_\alpha(\mathbf{C}, \boldsymbol{\Gamma}_\alpha)}{\partial \mathbf{C}} \mathbf{F}^{\mathrm{T}} \right]\end{aligned} \tag{3.7}$$

if and only if the following inequality holds:

$$\Pi^i_{\mathrm{int}} = -\sum_{\alpha=1}^{m} \frac{\partial \Upsilon_\alpha(\mathbf{C}, \boldsymbol{\Gamma}_\alpha)}{\partial \boldsymbol{\Gamma}_\alpha} : \dot{\boldsymbol{\Gamma}}_\alpha = \sum_{\alpha=1}^{m} \mathbf{Q}_\alpha : \dot{\boldsymbol{\Gamma}}_\alpha \geq 0, \tag{3.8}$$

expressing the Clausius–Duhem form of the second law of thermodynamics for the internal dissipation Π^i_{int}, as a function of the internal strain rates $\dot{\boldsymbol{\Gamma}}_\alpha$, where the : operator indicates the double contraction between tensors. Such a fundamental inequality must be satisfied by a suitable set of evolution equations for the non-equilibrium stresses $\mathbf{Q}_\alpha$, requiring that $\mathbf{Q}_\alpha|_{t\to\infty}$ vanishes in the state of thermodynamic equilibrium.

The simplest mechanical description for the viscous behaviour of a living cell is given by the Maxwell model, leading to the following evolution equation:

$$\dot{\mathbf{Q}}_\alpha + \frac{\mathbf{Q}_\alpha}{\tau_\alpha} = \frac{\mathrm{d}}{\mathrm{d}t}\left(2\frac{\partial \psi^i_\alpha(\mathbf{C})}{\partial \mathbf{C}}\right), \tag{3.9}$$

where τ_α is the typical relaxation time, $\psi^i_\alpha(\mathbf{C})$ is the free energy corresponding to the α dissipation process and $\mathbf{Q}_\alpha|_{t=0} = 2(\partial \psi^i_\alpha(\mathbf{C})/\partial \mathbf{C})|_{t=0}$.

Recent experimental studies on living cells under dynamic loading have demonstrated that the viscoelastic behaviour of the cytoskeleton cannot be fully captured by a single relaxation time. The dynamic rheological properties of cells were reported using power-law structural damping models, exhibiting a continuum spectrum of relaxation times (Lim *et al.* 2006). A discrete approximation of such experimental behaviour can be proposed by considering the proper number of Maxwell models with different relaxation times in parallel. However, a single Maxwell model, having a relaxation time corresponding to the higher value determined in experimental tests, can be used for the purpose of our analysis. Such longest relaxation time has been reported to be in the range 10–40 s for different cell kinds (Jülicher *et al.* 2007), allowing us to define an appropriate time limit after which the viscous contribution can be neglected and a state of thermodynamic equilibrium can be assumed.

From the constitutive viewpoint, each cell family i in the following is treated at its thermodynamic equilibrium as a composite hyperelastic material, so that its strain energy function ψ^i_{eq} can be decomposed into the sum of an isotropic term ψ^i_{ISO} and an anisotropic term ψ^i_{ANISO} as follows (Gasser *et al.* 2006):

$$\psi^i_{\mathrm{eq}}(\mathbf{C},\mathbf{A}^i)=\psi^i_{\mathrm{ISO}}[I_1(\mathbf{C}),I_2(\mathbf{C})]+\psi^i_{\mathrm{ANISO}}[(\mathbf{C},\mathbf{A}^i)], \tag{3.10}$$

where I_k are the kth invariants of the tensor $\mathbf{C}$ $(k=1,2,3)$, and the incompressibility condition is expressed by means of the internal constraint $C(\mathbf{F})=[I_3(\mathbf{F})-1]=0$.

Constitutive relationships accounting for anisotropy are far more complex than isotropic ones, being difficult to describe by a unified theory. A particular case of anisotropy, *viz.* the directional reinforcement over an isotropic matrix, is often encountered in the finite deformations of composite materials. Given $\mathbf{a}^i_0$ the (reference) unit vector indicating the direction, obtained by homogenization of single fibres, of the anisotropic reinforcement within the cell type i, the strain energy function must add a dependence on the structural tensor $\mathbf{A}^i=\mathbf{a}^i_0\otimes\mathbf{a}^i_0$, as expressed in equation (3.10). A mechanical theory of anisotropic reinforcements has been proposed for fibrous materials, which adds a set of pseudo-invariants describing the directional reinforcement. The pseudo-invariants of $\mathbf{C}$ and $\mathbf{A}^i$ define the stretch measure along fibre reinforcement, being defined as $I_4(\mathbf{C},\mathbf{A}^i)=\mathbf{a}^i_0\cdot\mathbf{C}\mathbf{a}^i_0$ and $I_5(\mathbf{C},\mathbf{A}^i)=\mathbf{a}^i_0\cdot\mathbf{C}^2\mathbf{a}^i_0$. The Cauchy stress tensor for a fibre-reinforced, *incompressible* material can be expressed as (Ciarletta *et al.* 2008)

$$\begin{aligned}\boldsymbol{\sigma}^i_{\mathrm{eq}}=2\Bigg[&\left(\frac{\partial\psi^i_{\mathrm{eq}}}{\partial I_1}+I_1\frac{\partial\psi^i_{\mathrm{eq}}}{\partial I_2}\right)\mathbf{b}-\frac{\partial\psi^i_{\mathrm{eq}}}{\partial I_2}\mathbf{b}^2-q^i\mathbf{I}\\&+\frac{\partial\psi^i_{\mathrm{eq}}}{\partial I_4}\mathbf{F}\mathbf{a}_0\cdot\mathbf{F}\mathbf{a}_0+\frac{\partial\psi^i_{\mathrm{eq}}}{\partial I_5}\left(\mathbf{F}\mathbf{a}^i_0\otimes\mathbf{b}\mathbf{F}\mathbf{a}^i_0+\mathbf{F}\mathbf{a}^i_0\mathbf{b}\otimes\mathbf{F}\mathbf{a}^i_0\right)\Bigg],\end{aligned} \tag{3.11}$$

where q^i is the Lagrange multiplier to restore the incompressibility condition, $C(\mathbf{F})=0$. In the case of multiple directional reinforcements, further pseudo-invariants must be added to account for anisotropic mechanical coupling. The mathematical treatment of this coupling has been developed by Spencer (1984), providing an extensive theory of multiple reinforcements.

The biophysical literature is filled with studies concerning the mathematical representation of the mechanical behaviour of soft biological networks undergoing finite strains. Theories for determining the force–extension response of semiflexible filaments have recently been proposed, accounting for thermal fluctuations and elastic bending energy (Karpeev *et al.* 2007; Purohit *et al.* 2008). The strain energy density of a network of F-actin has been related to the dynamics of single molecules and to the overall density of filaments in an idealized network connectivity and structure, demonstrating that cross-link concentration plays a major role in determining the mechanical stiffness of the network (Gardel *et al.* 2004). A generic competition exists between filament stretching and cross-link shearing, leading to distinct scaling behaviours with respect to bundle dimensions and molecular composition (Bathe *et al.* 2008).

In order to define suitable mathematical functions for the strain energy at thermodynamic equilibrium, besides the requirements of growth compatibility and material frame indifference, the issue of material stability has to be taken into account for maintaining integrity during elastic deformations (Schröder & Neff 2003). Possible criteria for stability may be derived by imposing the strong-ellipticity condition or the polyconvexity of the strain energy function (Ehret & Itskov 2007). Although beyond the scope of this study, these mathematical arguments are fundamental for demonstrating a global existence theory for the elastic solution.

(*c*) *Balance principles and axisymmetric solution*

The elastic solution for the problem of the elongation process of the *C. elegans* embryo is defined as the displacement field associated with the deformation gradient $\mathbf{F}$ that is compatible with the kinematic requirements and that fulfils all of the balance principles for each biological constituent, through the introduction of the proposed constitutive equations. Denoting the set of cylindrical coordinates in the initial configuration by (R, Θ, Z), the solution of the elastic problem is the compatible and self-equilibrated (in the sense mentioned above) position field $r = r(R, \Theta, Z)$, $\theta = \theta(R, \Theta, Z)$, $z = z(R, \Theta, Z)$ in the current configuration. The determination of an analytical solution requires the introduction of few basic assumptions to reduce the complexity of the elastic problem. Adopting the hypothesis of the continuum theory, the process of embryo elongation proceeds at approximately $100\,\mu\mathrm{m\,h}^{-1}$ for a period of about 2 h (Ding *et al.* 2004), and it can be assumed to occur in a quasi-static manner.

General assumptions about the symmetry properties of the elastic solution can be considered to impose the geometrical properties of a compatible deformation field. As the embryo elongates by a factor of four, at a reasonable distance from both ends (at a distance about that of the deformed radius), the deformation of the embryo can be assumed not to be dependent on Z, with $r = r(R, \Theta)$ and $\theta = \theta(R, \Theta)$. Moreover, the cylindrical section remains planar, so that $z = z(Z)$. The experimental observations of the embryonic elongation process allow us to consider the hypothesis that the sections of embryo (with respect to the deformed axis of symmetry) remain circular in the deformed configurations, as shown in figure 3. The global incompressibility requirement for each cell family i can be

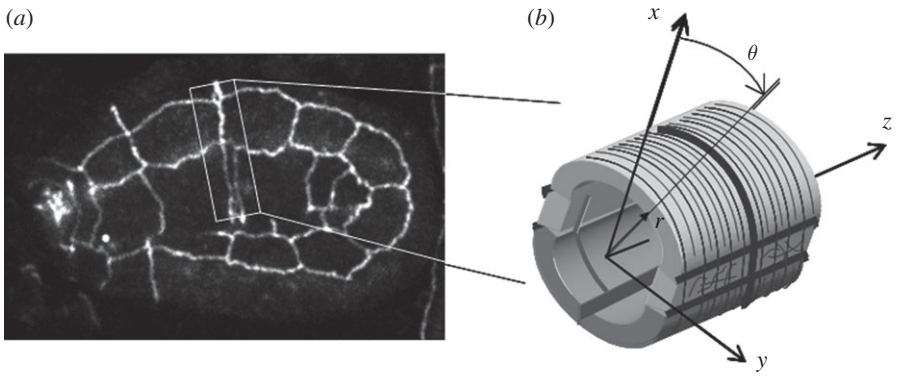

Figure 3. (*a*) Elongated *C. elegans* embryo at later stage and (*b*) geometrical model of epithelial cells with indication of internal structure (grey line, MTs; thin black line, F-actin; thick black line, adherens junctions).

expressed as $(i = \mathrm{d}, \mathrm{l}, \mathrm{v})$

$$[(r_1 + h^i)^2 - r_1^2](\theta^i_{\mathrm{fin}} - \theta^i_{\mathrm{in}})[z^i(L) - z^i(0)] = [(R_1 + H^i)^2 - R_1^2](\Theta^i_{\mathrm{fin}} - \Theta^i_{\mathrm{in}})L, \tag{3.12}$$

while the continuity condition of the embryonic deformation at the interfaces between different cell families imposes that

$$\sum_i (\theta^i_{\mathrm{fin}} - \theta^i_{\mathrm{in}}) = 2\pi \quad \theta^{\mathrm{d}}_{\mathrm{fin}} = \theta^{\mathrm{l}}_{\mathrm{in}} \quad \text{and} \quad \theta^{\mathrm{l}}_{\mathrm{fin}} = \theta^{\mathrm{v}}_{\mathrm{in}}, \tag{3.13}$$

$$\frac{z^j(L) - z^j(0)}{L} = \frac{z^k(L) - z^k(0)}{L}, \quad j, k = (\mathrm{d}, \mathrm{v}, \mathrm{l}). \tag{3.14}$$

Here r_1 and R_1 indicate the internal radius in the deformed and the undeformed configurations, and θ^i_{in} and θ^i_{fin} are the space-dependent functions expressing the initial and final angular coordinates for each cell family in the deformed configuration.

Similarly, the global incompressibility and continuity conditions applied to the inside biological matter are given by

$$r_1^2[z^{\mathrm{m}}(L) - z^{\mathrm{m}}(0)] = R_1^2 L, \tag{3.15}$$

$$\frac{z^{\mathrm{m}}(L) - z^{\mathrm{m}}(0)}{L} = \frac{z^i(L) - z^i(0)}{L}, \quad i = (\mathrm{d}, \mathrm{l}, \mathrm{v}). \tag{3.16}$$

An admissible solution of the elastic problem is given by the following deformation fields for the inside mass m, and the generic cell family i:

$$r^{\mathrm{m}} = \frac{R}{\sqrt{\lambda_z}}, \quad \theta^{\mathrm{m}} = \Theta^{\mathrm{m}} \quad \text{and} \quad z^{\mathrm{m}} = \lambda_z Z, \tag{3.17}$$

$$r^i = \sqrt{\frac{R^2}{G^i \lambda_z} + \frac{(R_2^i r_1)^2 - (R_1 r_2^i)^2}{(R_2^i)^2 - R_1^2}}, \quad \theta^i = G^i \Theta + J^i \quad \text{and} \quad z^i = \lambda_z Z. \tag{3.18}$$

Here $R_2^i = (R_1 + H^i)$, $r_2^i = (r_1 + h^i)$ and the constants G^i and J^i express a piecewise uniform deformation field with a uniform longitudinal embryonic stretch, λ_z.

The deformation tensors associated with such admissible deformation fields are the following:

$$\mathbf{F}^{\mathrm{m}} = \begin{bmatrix} R^{\mathrm{m}}/\lambda_z r^{\mathrm{m}} & 0 & 0 \\ 0 & r^{\mathrm{m}}/R^{\mathrm{m}} & 0 \\ 0 & 0 & \lambda_z \end{bmatrix} \quad \text{and} \quad \mathbf{F}^i = \begin{bmatrix} R^i/\lambda_z G^i r^i & 0 & 0 \\ 0 & (r^i/R^i)\, G^i & 0 \\ 0 & 0 & \lambda_z \end{bmatrix}, \tag{3.19}$$

which respect the local incompressibility constraints, $C(\mathbf{F}^\delta) = \det \mathbf{F}^\delta - 1 = 0$, where $\delta = (\mathrm{m}, \mathrm{d}, \mathrm{l}, \mathrm{v})$. Through the constitutive relationships in equations (3.5), (3.7) and (3.10), the stress fields inside the embryo at thermodynamic equilibrium are given by

$$\begin{aligned} \boldsymbol{\sigma}^\delta &= \boldsymbol{\sigma}^\delta_{\mathrm{act}}(\Delta\mu, \mathbf{p}) + \boldsymbol{\sigma}^\delta_{\mathrm{eq}}(\mathbf{C}^\delta, \mathbf{A}^\delta) \\ &= -\zeta\, \Delta\mu^\delta \cdot \mathbf{e}_\theta \otimes \mathbf{e}_\theta + 2\mathbf{F}^\delta \frac{\partial(\psi^\delta_{\mathrm{ISO}}(\mathbf{C}^\delta) + \psi^\delta_{\mathrm{ANISO}}(\mathbf{C}^\delta, \mathbf{A}^\delta))}{\partial \mathbf{C}^\delta} \mathbf{F}^{\mathrm{T}}_\delta - q^\delta \mathbf{I}, \end{aligned} \tag{3.20}$$

$$\boldsymbol{\sigma}^\delta = \boldsymbol{\Sigma}^\delta - q^\delta \mathbf{I} = \begin{bmatrix} \Sigma^\delta_{rr} - q^\delta & 0 & 0 \\ 0 & \Sigma^\delta_{\theta\theta} - q^\delta & 0 \\ 0 & 0 & \Sigma^\delta_{zz} - q^\delta \end{bmatrix}, \tag{3.21}$$

and the following boundary conditions have to be imposed:

$$\sigma^i_{rr}(r_1) = \sigma^{\mathrm{m}}_{rr}(r_1) \quad \text{and} \quad \sigma^i_{rr}(r_2^i) = 0 \quad (i = \mathrm{d}, \mathrm{v}, \mathrm{l}) \tag{3.22}$$

Applying the momentum balance principles for the body, the equilibrium imposes the following equalities to the Cauchy stress tensor $\boldsymbol{\sigma}$ and the first Piola stress tensor $\mathbf{P}$:

$$\operatorname{div} \boldsymbol{\sigma} + \mathbf{m} = \rho \dot{\mathbf{v}}, \tag{3.23}$$

$$\operatorname{Div} \mathbf{P} + \mathbf{M} = \rho_0 \dot{\mathbf{V}}, \tag{3.24}$$

where (div, $\mathbf{m}$, ρ) and (Div, $\mathbf{M}$, ρ_0) are the divergence operator, the volume body force and the density in the current and reference configuration, respectively. The slow elongation rate is supposed to create a negligible inertial force for the embryo. The body forces related to the mass and the friction effects are also considered irrelevant compared with the stress exerted in the elongation process.

The reduced equilibrium conditions, $\operatorname{div}(\boldsymbol{\sigma}^\delta) = 0$, are simplified by the fact that the stress fields are diagonal. For the stresses acting in the plane (r, θ), the equilibrium equation can be expressed as

$$\frac{\partial(r \cdot \sigma^\delta_{rr})}{\partial r} - \sigma^\delta_{\theta\theta} = 0. \tag{3.25}$$

For the inside biological matter, the problem of stress singularity at $r = 0$ is avoided if and only if $\Sigma^{\mathrm{m}}_{rr} = \Sigma^{\mathrm{m}}_{\theta\theta}$, where q^{m} is a constant parameter to be determined from the boundary condition at $r = r_1$: $\sigma^i_{rr}(r_1) = \sigma^{\mathrm{m}}_{rr}(r_1)$.

Given the hollow geometry of the embryonic epidermis, the equilibrium equation for the stress admits the variability of q^i along the radius for the generic cell type i. The value of the hydrostatic pressure $q^i(r)$ is given, from equation (3.25), by

$$q^i(r) = \Sigma^i_{rr} + \int_{r_1}^{r} \frac{\Sigma^i_{rr} - \Sigma^i_{\theta\theta}}{r^i} \mathrm{d}r^i + C^i_0, \tag{3.26}$$

where C^i_0 is a constant that can be determined from the boundary condition at $r = r^i_2 : \sigma^i_{rr}(r^i_2) = 0$.

Finally, let us imagine making a cut in a section perpendicular to the deformed symmetry axis. The equilibrium equations for the whole embryo with respect to the deformed longitudinal direction are given by

$$\sum_i \int_{r_1}^{r_2^i} \int_{\theta^i_{\mathrm{in}}}^{\theta^i_{\mathrm{fin}}} \sigma^i_{zz} r \cdot \mathrm{d}r \, \mathrm{d}\theta + \int_0^{r_1} \int_0^{2\pi} \sigma^{\mathrm{m}}_{zz} r \cdot \mathrm{d}r \, \mathrm{d}\theta = 0, \tag{3.27}$$

$$\sum_i \int_{r_1}^{r_2^i} \int_{\theta^i_{\mathrm{in}}}^{\theta^i_{\mathrm{fin}}} \sigma^i_{zz} r^2 \cos\theta \cdot \mathrm{d}r \, \mathrm{d}\theta = 0. \tag{3.28}$$

The elastic solution is the set of parameters (G^i, J^i, λ_z) describing the deformation field of the elongating embryo: it is given by the system of nonlinear equations made by the constitutive relationships in equations (3.5), (3.7) and (3.10), the incompressibility conditions in equation (3.12), the continuity of deformation in equations (3.13) and (3.14), and the equilibrium equations for the embryo in equations (3.27) and (3.28).

4. A particular analytical solution: the mechanical role of cellular filaments during embryogenesis

In order to get an easier analytical expression of the solution for the biomechanical model for the *C. elegans* embryo, we focus on solving the simplified problem where the dorsal and ventral cell rows have the same geometrical distribution and the same mechanical properties. This assumption adds another plane of symmetry to the problem (thus, reducing the complexity of the system of nonlinear equations), and it allows an analytical description of the role of the directionally oriented cellular filaments in the determination of the final shape of the elongating embryo.

For simplicity, the isotropic strain energy functions of the cell families and of the inside biological matter are considered as neo-Hookean materials, as follows:

$$\psi^{\delta}_{\mathrm{ISO}}(\mathbf{C}^{\delta}) = c^{\delta}_1 [I_1(\mathbf{C}^{\delta}) - 3], \tag{4.1}$$

where c^{δ}_1 $(\delta = \mathrm{d}, \mathrm{l}, \mathrm{v}, \mathrm{m})$ are positive material parameters. Moreover, the inside mass is modelled as a passive isotropic material, neglecting the mechanical effect of anisotropic structures that could be detected inside.

The passive anisotropic response of the epithelial cells at thermodynamic equilibrium is mainly caused by the spatial orientation of the MTs. Continuum elastic beam models of MT buckling in living cells have demonstrated that the buckling wavelength is determined by the interplay with the nonlinear elastic biopolymeric network in the cell, while the buckling amplitude and growth rate are set by the viscous properties of the cytosol (Li 2008). In particular, non-equilibrium analysis of the MTs' buckling spectrum has reported that even large compressive forces between cells cause short-wavelength MT fluctuations, while the long-wavelength modes are frozen in by the constraints given by the surrounding cellular network (Brangwynne *et al.* 2007, 2008). The dynamic behaviour of the short-wavelength regime deviates from the predictions of the worm-like chain model, resulting in a complex dependence of the bending stiffness on the filament length (Taute *et al.* 2008). Such a length dependence of flexural rigidity is attributed to the low shear modulus of MTs (six orders of magnitude lower than the longitudinal modulus) using a Timoshenko-beam model, predicting that MTs of different lengths are able to sustain almost equal maximum compressive force against column buckling (Shi *et al.* 2008). In general, bundling of MTs within epithelial cells determines a strong mechanical reinforcement along a preferred direction. MTs stiffen against longitudinal elongation in lateral cells, while they resist contractile myosin forces in the circumferential direction, having a bending stiffness depending on the strength of cross-linkers between individual filaments. The expressions for the anisotropic response of distributed MT network in epithelial cells are simplified in the following in order to obtain an analytical solution for the elastic problem. The anisotropic strain energy functions are described by means of a neo-Hookean reinforcement law in hyperelasticity (Qiu & Pence 1997*a*)

$$\psi^{\mathrm{d}}_{\mathrm{ANISO}}(\mathbf{C}^{\delta},\mathbf{A}^{\mathrm{d}}) = c^{\mathrm{d}}_{4\theta}[I_4(\mathbf{C}^{\delta},\mathbf{e}_\theta\otimes\mathbf{e}_\theta)-1]^2, \tag{4.2}$$

$$\psi^{\mathrm{l}}_{\mathrm{ANISO}}(\mathbf{C}^{\delta},\mathbf{A}^{\mathrm{l}}) = c^{\mathrm{l}}_{4\theta}[I_4(\mathbf{C}^{\delta},\mathbf{e}_\theta\otimes\mathbf{e}_\theta)-1]^2 + c^{\mathrm{l}}_{4z}[I_4(\mathbf{C}^{\delta},\mathbf{e}_z\otimes\mathbf{e}_z)-1]^2, \tag{4.3}$$

where $c^{\mathrm{d}}_{4\theta}$ and $c^{\mathrm{l}}_{4\theta}$ are the neo-Hookean reinforcement coefficients of dorsal and lateral cells in the circumferential direction and c^{l}_{4z} is the tensile reinforcement coefficient in the longitudinal direction for the lateral cells. Equations (4.2) and (4.3) are considered as illustrative constitutive relationships of directional reinforcements in nonlinear elasticity, referring to the work of Qiu & Pence (1997*b*) for the limitations imposed by the elastic stability requirements.

The radial displacement fields from the incompressibility conditions in equation (3.12) can be expressed as

$$r^{\mathrm{m}} = \frac{R^{\mathrm{m}}}{\sqrt{\lambda_z}} \quad \text{and} \quad r^{i} = \sqrt{\frac{1}{G^i\lambda_z}(R^i)^2 + \frac{G^i-1}{G^i\lambda_z}R_1^2} \quad (i=\mathrm{d},\mathrm{l}). \tag{4.4}$$

The continuity of the circumferential deformation for the epidermis imposes that

$$G^{\mathrm{l}} = \frac{\pi/2 - G^{\mathrm{d}}\Theta^{\mathrm{d}}_{\mathrm{fin}}}{\pi/2-\Theta^{\mathrm{d}}_{\mathrm{fin}}}, \quad J^{\mathrm{d}}=0 \quad \text{and} \quad J^{\mathrm{l}} = \frac{\pi}{2}(G^{\mathrm{l}}-1). \tag{4.5}$$

From equations (4.2) and (4.3), the components of the stress tensor $\boldsymbol{\Sigma}^i$, defined in equation (3.21), can be written for the epithelial cells of the embryo as $(i = \mathrm{d}, \mathrm{l})$

$$\Sigma^i_{rr} = 2c^i_1 \left(\frac{R^i}{r^i} \frac{1}{G^i \lambda_z} \right)^2, \tag{4.6}$$

$$\Sigma^i_{\theta\theta} = \left(\frac{r^i}{R^i} G^i \right)^2 \left[2c^i_1 - 2c^i_{4\theta} + 2c^i_{4\theta} \left(\frac{r^i}{R^i} G^i \right)^2 \right] - \zeta \Delta\mu^i, \tag{4.7}$$

$$\Sigma^{\mathrm{d}}_{zz} = 2c^{\mathrm{d}}_1 \lambda_z^2 \quad \text{and} \quad \Sigma^{\mathrm{l}}_{zz} = \lambda_z^2 [2c^{\mathrm{l}}_1 + 2c^{\mathrm{l}}_{4z}(\lambda_z^2 - 1)]. \tag{4.8}$$

From equation (3.26), the hydrostatic pressures $q^i(r)$ in the epithelial cells can be written as:

$$q^i(r) = 2c^i_1 \left(\frac{R}{r} \frac{1}{G^i \lambda_z} \right)^2 - \int_r^{r^i_2} \frac{2c^i_1 \{ [(R^i/r^i)(1/G^i\lambda_z)]^2 - [(r^i/R^i)\, G^i]^2 \}}{r^i} \mathrm{d}r^i.$$
$$+ \int_r^{r^i_2} \frac{2c^i_{4\theta} [(r^i/R^i)\, G^i]^2 \{ [(r^i/R^i)\, G^i]^2 - 1 \} + \zeta \Delta\mu^i}{r^i} \mathrm{d}r^i. \tag{4.9}$$

The terms under the integration in equation (4.9) can be rewritten, using equations (3.19) and (4.4), as

$$\int_r^{r^i_2} \frac{2c^i_1 ((R^i/r^i)(1/G^i\lambda_z))^2}{r^i} \mathrm{d}r^i = \int_r^{r^i_2} 2c^i_1 \frac{(r^i)^2 - R_1^2 (G^i - 1)}{(G^i \lambda_z)(r^i)^3} \mathrm{d}r^i$$
$$= \frac{2c^i_1}{G^i \lambda_z} \left[\ln \frac{r^i_2}{r} + \frac{R_1^2}{2} (G^i - 1) \left(\frac{1}{(r^i_2)^2} - \frac{1}{r^2} \right) \right], \tag{4.10}$$

$$\int_r^{r^i_2} (2c^i_1 - 2c^i_{4\theta}) \frac{(G^i)^2 r^i}{(R^i)^2} \mathrm{d}r^i = \int_R^{R^i_2} (2c^i_1 - 2c^i_{4\theta}) \frac{G^i}{\lambda_z R^i} \mathrm{d}R^i = (2c^i_1 - 2c^i_{4\theta}) \frac{G^i}{\lambda_z} \ln \frac{R^i_2}{R} \tag{4.11}$$

and

$$\int_r^{r^i_2} 2c^i_{4\theta} (G^i)^4 \frac{(r^i)^3}{(R^i)^4} \mathrm{d}r^i = \int_R^{R^i_2} \frac{2c^i_{4\theta} (G^i)^3}{\lambda_z} \frac{(r^i)^2}{(R^i)^3} \mathrm{d}R^i$$
$$= \frac{2c^i_{4\theta} (G^i)^2}{\lambda_z^2} \ln \frac{R^i_2}{R} - \frac{c^i_{4\theta} (G^i)^2 (G^i - 1)}{\lambda_z^2} R_1^2 \left(\frac{1}{R^i_2} - \frac{1}{R^2} \right). \tag{4.12}$$

From equations (4.10)–(4.12), the hydrostatic pressures in equation (4.9) become

$$\begin{aligned} q^i(r) = {} & 2c_1^i\left(\frac{R}{r}\frac{1}{G^i\lambda_z}\right)^2 - \frac{2c_1^i}{G^i\lambda_z}\left[\ln\frac{r_2^i}{r} + \frac{R_1^2}{2}(G^i-1)\left(\frac{1}{(r_2^i)^2}-\frac{1}{r^2}\right)\right] \\ & - \zeta\,\Delta\mu^i \ln\frac{r_2^i}{r} + (2c_1^i - 2c_{4\theta}^i)\frac{G^i}{\lambda_z}\ln\frac{R_2^i}{R} + \frac{2c_{4\theta}^i(G^i)^2}{\lambda_z^2}\ln\frac{R_2^i}{R} \\ & - \frac{c_{4\theta}^i(G^i)^2(G^i-1)}{\lambda_z^2}R_1^2\left(\frac{1}{(R_2^i)^2}-\frac{1}{R_2^i}\right). \end{aligned} \tag{4.13}$$

For what concerns the biological matter inside the embryonic epidermis, the constitutive relationships from equation (4.1) define its stress functions as

$$\Sigma_{rr}^{\mathrm{m}} = \Sigma_{\theta\theta}^{\mathrm{m}} = 2c_1^{\mathrm{m}}\frac{1}{\lambda_z}, \tag{4.14}$$

$$\Sigma_{zz}^{\mathrm{m}} = 2c_1^{\mathrm{m}}\lambda_z^2, \tag{4.15}$$

while the hydrostatic term q^{m} has a constant value that can be recovered from the boundary condition at $r = r_1$,

$$q^{\mathrm{m}} = 2c_1^{\mathrm{m}}\frac{1}{\lambda_z} - \Sigma_{rr}^{\mathrm{d}}(r_1) + q^{\mathrm{d}}(r_1) = 2c_1^{\mathrm{m}}\frac{1}{\lambda_z} - \Sigma_{rr}^{\mathrm{l}}(r_1) + q^{\mathrm{l}}(r_1). \tag{4.16}$$

Furthermore, the equilibrium in the longitudinal direction in equation (3.27) imposes that

$$\begin{aligned} & \int_{r_1}^{r_2^{\mathrm{d}}}\int_0^{G^{\mathrm{d}}\Theta_{\mathrm{fin}}^{\mathrm{d}}}[\Sigma_{zz}^{\mathrm{d}} - q^{\mathrm{d}}(r)]r\,\mathrm{d}r\,\mathrm{d}\theta + \int_{r_1}^{r_2^{\mathrm{l}}}\int_{G^{\mathrm{d}}\Theta_{\mathrm{fin}}^{\mathrm{d}}}^{\pi/2}[\Sigma_{zz}^{\mathrm{l}} - q^{\mathrm{l}}(r)]r\,\mathrm{d}r\,\mathrm{d}\theta \\ & \quad + \int_0^{r_1}\int_0^{\pi/2}[\Sigma_{zz}^{\mathrm{m}} - q^{\mathrm{m}}]\,r\,\mathrm{d}r\,\mathrm{d}\theta = 0. \end{aligned} \tag{4.17}$$

Developing the integral terms in equation (4.17), they can be written as

$$\begin{aligned} & \int_{r_1}^{r_2^i}[\Sigma_{zz}^i - q^i(r)]r\,\mathrm{d}r \\ & = \frac{1}{2}\Sigma_{zz}^i[(r_2^i)^2 - r_1^2] - \frac{2c_1^i}{G^i\lambda_z}\left[\frac{1}{2}[(R_2^i)^2 - R_1^2] + \frac{(G^i-1)}{G^i\lambda_z}R_1^2\ln\frac{r_1}{r_2^i}\right] \\ & \quad + \left(\frac{2c_1^i}{G^i\lambda_z} + \zeta\,\Delta\mu^i\right)\left[\frac{1}{4}[(r_2^i)^2 - r_1^2] + \frac{r_1^2}{2}\ln\frac{r_1}{r_2^i}\right] \\ & \quad - \frac{c_1^i}{G^i\lambda_z}R_1^2(G^i-1)\left[\frac{1}{2(r_2^i)^2}[(r_2^i)^2 - r_1^2] + \ln\frac{r_1}{r_2^i}\right] \\ & \quad + \frac{1}{\lambda_z^2}\left[2c_1^i + 2c_{4\theta}^i\left(-1 + \frac{G^i}{\lambda_z}\right)\right]\left[\frac{1}{4}[(R_2^i)^2 - R_1^2] + \frac{R_1^2}{2}\ln\frac{R_1}{R_2^i}\right] \\ & \quad + \frac{c_{4\theta}^i(G^i)^2(G^i-1)}{\lambda_z^2}R_1^2\left[\frac{1}{2(R_2^i)^2}[(r_2^i)^2 - r_1^2] + \frac{1}{G^i\lambda_z}\ln\frac{R_1}{R_2^i}\right] \end{aligned} \tag{4.18}$$

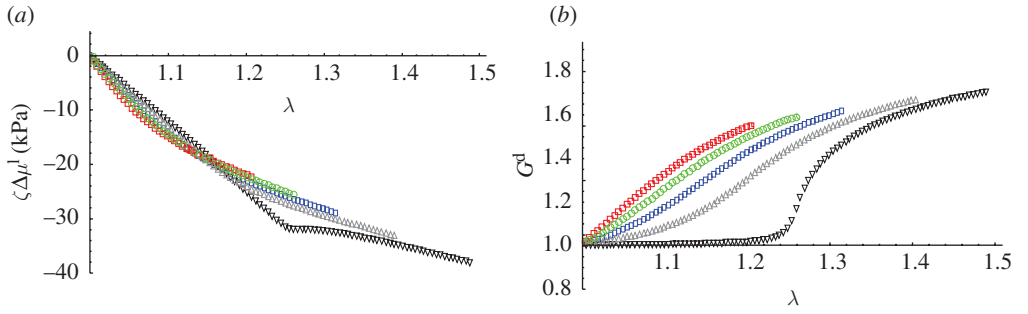

Figure 4. Theoretical predictions of the continuum model, neglecting the mechanical response of MTs ($c^{\mathrm{d}}_{4\theta} = c^{\mathrm{l}}_{4\theta} = c^{\mathrm{l}}_{4z} = 0$): (*a*) chemical activity $\zeta\,\Delta\mu^{\mathrm{l}}$ of the actin–myosin complex in lateral cells and (*b*) angular extension of dorsal cells G^{d}, shown versus the embryonic stretch λ and at different activation levels of $\zeta\,\Delta\mu^{\mathrm{d}}(\zeta\,\Delta\mu^{\mathrm{d}}/\zeta\,\Delta\mu^{\mathrm{l}} = 0$, red squares; 0.25, green circles; 0.50, blue rectangles; 0.75, grey triangles; and 1.00, black inverted triangles). The curves are calculated for $R_1 = 8\,\mu\mathrm{m}$, $H^{\mathrm{l}} = H^{\mathrm{d}} = 2\,\mu\mathrm{m}$, $\Theta_{\mathrm{fin}} = \pi/4$ and $c^{\mathrm{d}}_1 = 2c^{\mathrm{l}}_1 = 4c^{\mathrm{m}}_1 = 6\,\mathrm{kPa}$.

and

$$\int_0^{r_1}\int_0^{\pi/4} [\Sigma^{\mathrm{m}}_{zz} - q^{\mathrm{m}}]\, r\,\mathrm{d}r\,\mathrm{d}\theta = \frac{\pi}{4} r_1^2 \left[2c^{\mathrm{m}}_1 \left(\lambda_z^2 - \frac{1}{\lambda_z} \right) - \Sigma^{\mathrm{d}}_{rr}(r_1) + q^{\mathrm{d}}(r_1) \right]$$
$$= \frac{\pi}{4} r_1^2 \left[2c^{\mathrm{m}}_1 \left(\lambda_z^2 - \frac{1}{\lambda_z} \right) - \Sigma^{\mathrm{l}}_{rr}(r_1) + q^{\mathrm{l}}(r_1) \right]. \quad (4.19)$$

Let us rewrite the incompressibility and continuity conditions in equations (4.4) and (4.5) as follows:

$$r^{\mathrm{d}}_2 = \sqrt{\frac{1}{G^{\mathrm{d}}\lambda_z}(R^{\mathrm{d}}_2)^2 + \frac{G^{\mathrm{d}} - 1}{G^{\mathrm{d}}\lambda_z} R_1^2}, \quad r^{\mathrm{l}}_2 = \sqrt{\frac{1}{G^{\mathrm{l}}\lambda_z}(R^{\mathrm{l}}_2)^2 + \frac{G^{\mathrm{l}} - 1}{G^{\mathrm{l}}\lambda_z} R_1^2},$$
$$r_1 = \frac{R_1}{\sqrt{\lambda_z}} \quad \text{and} \quad G^{\mathrm{l}} = \frac{\pi/2 - G^{\mathrm{d}}\Theta^{\mathrm{d}}_{\mathrm{fin}}}{\pi/2 - \Theta^{\mathrm{d}}_{\mathrm{fin}}}. \quad (4.20)$$

Once the terms in equations (4.20) are substituted into the equilibrium equations (4.16) and (4.17), the resulting expressions report how the experimental measurements of the set $(G^{\mathrm{d}}, \lambda_z)$ during the elongation process, together with the data of the initial geometry of the embryo $(R_1, R^{\mathrm{d}}_2, R^{\mathrm{l}}_2, \Theta^{\mathrm{d}}_{\mathrm{fin}})$, allow us to study the mechanical role of cellular filaments during the elongation process of the embryo. In conclusion, the hyperelastic solution (i.e. the deformation field) for the embryonic elongation is given by the set of five kinematic parameters $(G^{\mathrm{d}}, G^{\mathrm{l}}, J^{\mathrm{d}}, J^{\mathrm{l}}, \lambda_z)$ that can be obtained by solving the system composed by the three equations describing the continuity conditions in equations (4.20) and by the two equilibrium equations for the stress fields in equations (4.16) and (4.17). Although the problem is well posed and a solution can be found, the analytical expression is difficult to achieve because the parameters are essentially involved in a non-algebraic way. As an example, a numerical solution of the continuum model has been calculated both for an isotropic ($c^{\mathrm{d}}_{4\theta} = c^{\mathrm{l}}_{4\theta} = c^{\mathrm{l}}_{4z} = 0$) and for

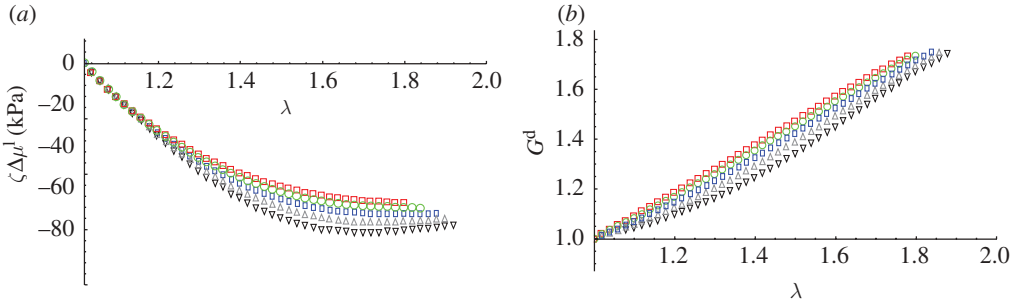

Figure 5. Theoretical predictions of the continuum model, including the anisotropic response of MTs ($c^{\mathrm{d}}_{4\theta} = 10c^{\mathrm{l}}_{4\theta} = 10c^{\mathrm{l}}_{4z} = 100\,\mathrm{kPa}$): (*a*) chemical activity $\zeta\Delta\mu^{\mathrm{l}}$ of the actin–myosin complex in lateral cells; and (*b*) angular extension of dorsal cells G^{d}, shown versus the embryonic stretch λ, and at different activation levels of $\zeta\Delta\mu^{\mathrm{d}}(\zeta\Delta\mu^{\mathrm{d}}/\zeta\Delta\mu^{\mathrm{l}} = 0$, red squares; 0.25, green circles; 0.50, blue rectangles; 0.75, grey triangles; and 1.00, black inverted triangles). The geometrical data and the other mechanical parameters are the same as in figure 4.

an anisotropic ($c^{\mathrm{d}}_{4\theta} = 10c^{\mathrm{l}}_{4\theta} = 10c^{\mathrm{l}}_{4z} = 100\,\mathrm{kPa}$) passive behaviour of the cells, as shown in figures 4 and 5. The curves show (*a*) the chemical activities $\zeta\Delta\mu^{i}$ of the actin–myosin complexes and (*b*) the angular extension G^{d} of dorsal cells as a function of the overall embryonic elongation λ_z. The limit of validity of the numerical solution has been fixed by setting the maximum outer radius of the deformed cells equal to the inner radius of the outer shell surrounding the embryo.

5. Discussion

The continuum model proposed in this study aims to derive an analytic description of the stress fields inside the *C. elegans* embryo during its elongation process. From a constitutive viewpoint, a free energy function for the embryonic cells has been defined in order to account both for the anisotropic contractile forces of myosin motors and for the passive mechanical behaviour of the cellular networks. The axisymmetric elastic solution of the elongation process at thermodynamic equilibrium is proposed by means of the incompressibility conditions, the continuity equations of the deformation fields and the balance principles for the embryonic cells. A particular analytical solution is derived for the simplified problem where dorsal and ventral cells have the same mechanical and geometrical properties. Using simplified expressions for the anisotropic strain energy functions, the geometry of the elongated embryo is related in an analytic way both to the chemical activities $\zeta\Delta\mu^{i}$ of the actin–myosin complexes and to the material parameters $c^{i}_{4\theta}$ and c^{i}_{4z} describing the compressive and tensile behaviours, respectively, of the MT reinforcements within epithelial cells. The predictions of the proposed model can be used to evaluate the biomechanical consistency of the elongation mechanisms suggested by the genetic analysis along with pharmacological experiments (Wissmann *et al.* 1997; Shelton *et al.* 1999; Piekny *et al.* 2003; Diogon *et al.* 2007; Quintin *et al.* 2008). The numerical results shown in figures 4 and 5 support the interpretation that the sole non-muscle myosin II contraction in the lateral epidermal cells (square, $\zeta\Delta\mu^{\mathrm{d}} = 0$) is able to trigger embryo shape changes by shortening the circumferential actin filaments

in those cells. Accordingly, if the volume of cells is kept constant during actin shortening, the lateral cells elongate along the antero-posterior axis. Meanwhile, the dorsal and ventral cells would stretch passively because they are tightly attached to lateral cells through adherens junctions. Moreover, the proposed model predicts that, if the non-muscle myosin II in dorsal/ventral cells is activated at a subsequent stage, a further embryonic elongation can be achieved. The relationship between the non-muscle myosin II contraction in epithelial cells and the overall embryonic elongation λ_z is shown in figures 4*b* and 5*b*.

Another important result of the derived elastic solution is that the passive mechanical response of the MT network within epithelial cells is essential to provoke a large finite stretch of the embryo from a contraction of circumferentially oriented myosin motors. Taking into account that MTs are stiff filaments that form bundles within epithelial cells, such bundled networks have anisotropic mechanical responses far stiffer than the bulk characteristics for several kinds of cell, ranging from 1 kPa to 1 MPa (Lulevich *et al.* 2006). The key mechanical effects due to the anisotropy of the MT networks can be identified by comparing the numerical results in figures 4 and 5. The elastic solution in figure 5 suggests that the MTs' anisotropy is fundamental to elongate the embryo up to a maximum stretch that is much higher than the one permitted by only considering an isotropic behaviour, as shown in figure 4. Furthermore, the role of MTs in the dorsal/ventral epidermis may be not only to drive overall elongation but also to evenly distribute forces between cells. The results suggest that the anisotropic properties of the MT networks may determine the change in the position of the adherens junction during the elongation process (i.e. the variation of the angular extension G^{d} over the embryonic stretch; figure 5*b*) from an asymmetric activation of non-muscle myosin II among the adjacent cell families. Moreover, the results shown in figure 5 point out that a potential role of MTs is to buffer/protect the embryo against small changes in the distribution and activity of myosin II, since even an important difference seems to have a rather neutral effect.

Some experimental data supporting these theoretical results are as follows: (i) actin depolymerizing drugs block the elongation process, whereas MT depolymerizing drugs induce abnormally shaped embryos that nevertheless can elongate to some degree (Labouesse 2006); (ii) mutations inactivating myosin II or its upstream regulator rho-kinase block the elongation process at an early stage (Shelton *et al.* 1999; Piekny *et al.* 2003); and (iii) a rho-GTPase activating protein acting in dorsal and ventral epidermal cells reduces myosin II activity in those cells (Diogon *et al.* 2007; Quintin *et al.* 2008). Moreover, the mechanical role of IFs in epithelial cells can be explained in the proposed model as a constraining effect that prevents MTs from long-wavelength buckling, contributing to the abnormal elongation of IF-deficient mutants.

Several limitations of the proposed model need to be discussed. Indeed, more recent genetic data suggest that the rho-kinase becomes dispensable midway through embryogenesis (Diogon *et al.* 2007), implying that the mechanism inducing F-actin shortening may not solely rely on a rho-kinase/myosin II pathway afterwards. More importantly, the model neglects the mechanical role of muscles, which become contractile slightly before embryos reach mid-elongation, being essential for completion of the elongation process (Williams & Waterson 1994). Mutants with defective muscles arrest morphogenesis at mid-elongation, as do mutants with defective hemidesmosomes

(Bosher *et al.* 2003; Woo *et al.* 2004). In addition, once muscles become active, as they are tightly attached to the epidermis at the level of hemidesmosomes, their contraction could potentially induce transient pulses of antero-posterior-directed tension that may induce a relevant deformation of the subcellular network. The specific cause for this phenotype remains unclear, but it points to the need to maintain a close coupling between muscles and the epidermis, and it again raises the possibility that cell shape changes may not solely rely on myosin II contractility stimulated by rho-kinase activity once muscles start to contract.

The theoretical predictions of the proposed model, if combined with the results of the experimental observations, may lead to notable advantages for the interpretation of the morphogenetic processes. Future developments of this study include the use of image processing on the *C. elegans* embryo, visualized with staining techniques, to measure the variation of the cell shape and of the subcellular structure for all the durations of the elongation process. Once the initial geometrical properties of the embryo are detected, such data can be used to build experimental curves of the deformation fields of each epithelial cell family between the current and the reference configurations, measured at each longitudinal stretch λ_z of embryonic elongation. These experimental data from normal and/or defective embryos can be compared with the theoretical predictions, with the aim to analyse the morphogenetic effect of each material parameter of the model. For example, experimental measurements of the values of G^{d} with growing λ_z can be used in equations (4.16) and (4.17) to quantify the effect of different concentrations of activated myosin, as reported in recent experimental observations (Diogon *et al.* 2007), and of an abnormal MT structure within epithelial cells. Further interesting information could arise from the analysis of the time-dependent spatial characteristics of the elongating embryo. In particular, the elongating embryo can be regarded from a biomechanical point of view as a hydrostatic skeleton where the sequential activation of myosin motors produces a peristaltic wave causing the elongation process. The dynamic properties of this propulsive mechanism could reveal some characteristics of the signal progression in actin–myosin sequential contraction, as well as determine the influence of bulk tribological properties and bending effects on the elongation characteristics. As outlined in the previous paragraphs, several testable predictions can be derived from the equations presented above. First, altering the relative amount of active myosin II in lateral versus dorsal/ventral epidermal cells should not alter the elongation efficiency until the twofold stage. Second, removing MTs in dorsal/ventral cells should be detrimental to elongation efficiency, especially if myosin II becomes limiting in dorsal/ventral cells. Third, modifying the anisotropic distribution of MTs should also alter elongation. Fourth, it will be important to determine if any internal organ, in particular the intestine, plays a passive role due to hydrostatic forces and incompressibility.

6. Conclusion

The elongation process in *C. elegans* embryos has been modelled in a continuum mechanics framework to study the morphogenetic effect of the structural cytoskeletal filaments in epithelial cells. This study has aimed at correlating the theoretical predictions of a biomechanical model with the biological

scenario proposed through genetic analysis and pharmacological experiments. The modelling of all forces active in each epidermal cell type has suggested that a non-muscle myosin II activation in lateral cells may trigger the embryonic elongation process, while a subsequent activation in dorsal/ventral cells may promote a further stretching. The proposed model has demonstrated that the mechanical ability of MTs to sustain compressive loads in these cells is essential to provoke a finite elongation from a differential contraction of circumferentially oriented actin filaments. Moreover, the compression of the internal content of the embryo has a key role in coordinating the overall epithelial morphogenesis of the embryo. The achieved results demonstrate a step towards validating existing biological observations to model the interplay between embryonic structure and mechanical force distribution during the elongation process. The proposed approach has the potential to drive progress on the challenge to define the feedback mechanisms of mechano-transduction during embryogenesis. Future studies will focus on incorporating the response of cytoskeletal filaments, using experimental techniques probing subcellular deformations, into a multi-scale constitutive description of epithelial cells. Relating the distribution of stress and strain fields within the embryo to the biophysical properties of the subcellular networks will allow for the study of the conversion of mechanical signals into biological and chemical responses. In conclusion, the combination of theoretical modelling in biomechanics with experimental methods in developmental biology represents a promising strategy towards the critical investigation of the pathways controlling the morphogenetic processes.

The authors are grateful to David Rodriguez for his kind help in the preparation of figures 1 and 3.

References

Bathe, M., Heussinger, C., Claessens, M., Bausch, A. R. & Frey, E. 2008 Cytoskeletal bundle mechanics. *Biophys. J.* **94**, 2955–2964. (doi:10.1529/biophysj.107.119743)

Boal, D. 2002 *Mechanics of the cell*. Cambridge, UK: Cambridge University Press.

Bosher, J. M., Hahn, B. S. & Legouis, R. 2003 The *Caenorhabditis elegans* vab-10 spectraplakin isoforms protect the epidermis against internal and external forces. *J. Cell Biol.* **161**, 757–768. (doi:10.1083/jcb.200302151)

Brangwynne, C. P., MacKintosh, F. C., Kumar, S., Geisse, N. A., Talbot, J., Mahadevan, L., Parker, K. K., Ingber, D. E. & Weitz, D. A. 2006 Microtubules can bear enhanced compressive loads in living cells because of lateral reinforcement. *J. Cell Biol.* **104**, 733–741. (doi:10.1083/jcb.200601060)

Brangwynne, C. P., MacKintosh, F. C. & Weitz, D. A. 2007 Force fluctuations and polymerization dynamics of intracellular microtubules. *Proc. Natl Acad. Sci. USA* **104**, 16 128–16 133. (doi:10.1073/pnas.0703094104)

Brangwynne, C. P., Koenderink, G. H., MacKintosh, F. C. & Weitz, D. A. 2008 Nonequilibrium microtubule fluctuations in a model cytoskeleton. *Phys. Rev. Lett.* **100**, 118104. (doi:10.1103/PhysRevLett.100.118104)

Caille, N., Thoumine, O., Tardy, Y. & Meister, J.-J. 2002 Contribution of the nucleus to the mechanical properties of endothelial cells. *J. Biomech.* **35**, 177–187. (doi:10.1016/S0021-9290(01)00201-9)

Callan-Jones, A. C., Joanny, J.-F. & Prost, J. 2008 Viscous-fingering-like instability of cell fragments. *Phys. Rev. Lett.* **100**, 258106. (doi:10.1103/PhysRevLett.100.258106)

Chaudhuri, O., Parekh, S. H. & Fletcher, D. A. 2007 Reversible stress softening of actin networks. *Nature* **445**, 295–298. (doi:10.1038/nature05459)

Chisholm, A. D. & Hardin, J. 2005 Epidermal morphogenesis. In *WormBook* (ed. The *C. elegans* Research Community). http://www.wormbook.org. (doi:10.1895/wormbook.1.35.1)

Ciarletta, P., Dario, P. & Micera, S. 2008 Pseudo-hyperelastic model of tendon hysteresis from adaptive recruitment of collagen type I fibrils. *Biomaterials* **29**, 764–770. (doi:10.1016/j.biomaterials.2007.10.020)

Dawes-Hoang, R. E., Parmar, K. M., Christiansen, A. E., Phelps, C. B., Brand, A. H. & Wieschaus, E. F. 2005 *folded gastrulation*, cell shape changes and the control of myosin localization. *Development* **132**, 4165–4178. (doi:10.1242/dev.01938)

Desai, A. & Mitchison, T. J. 1997 Microtubule polmerization dynamics. *Annu. Rev. Cell Dev. Biol.* **13**, 83–117. (doi:10.1146/annurev.cellbio.13.1.83)

Ding, M., Woo, W.-M. & Chisholm, A. D. 2004 The cytoskeleton and epidermal morphogenesis in *C. elegans*. *Exp. Cell Res.* **301**, 84–90. (doi:10.1016/j.yexcr.2004.08.017)

Diogon, M., Wissler, F., Quintin, S., Nagamatsu, Y., Sookhareea, S., Landmann, F., Hutter, H., Vitale, N. & Labouesse, M. 2007 The RhoGAP RGA-2 and LET-502/ROCK achieve a balance of actomyosin-dependent forces in *C. elegans* epidermis to control morphogenesis. *Development* **134**, 2469–2479. (doi:10.1242/dev.005074)

Ehret, A. E. & Itskov, M. 2007 A polyconvex hyperelastic model for fiber-reinforced materials in application to soft tissues. *J. Mater. Sci.* **42**, 8853–8863. (doi:10.1007/S10853-007-1812-6)

Fung, Y. C. 1981 *Biomechanics. Mechanical properties of living tissues*. New York, NY: Springer.

Gardel, M. L., Shin, J. H., MacKintosh, F. C., Mahadevan, L., Matsudaira, P. & Weitz, D.A. 2004 Elastic behaviour of cross-linked and bundled actin networks. *Science* **304**, 1301–1305. (doi:10.1126/science.1095087)

Gasser, T. C., Ogden, R. W. & Holzapfel, G. A. 2006 Hyperelastic modelling of arterial layers with distributed collagen fibre orientations. *J. R. Soc. Interf.* **3**, 15–35. (doi:10.1098/rsif.2005.0073)

Holzapfel, G. A. & Simo, J. C. 1996 A new viscoelastic constitutive model for continuous media at finite thermomechanical changes. *Int. J. Solids Struct.* **33**, 3019–3034. (doi:10.1016/0020-7683(95)00263-4)

Janmey, P. A., Hvidt, S., Kas, J., Lerche, D., Maggs, A., Sackmann, E., Schliwa, M. & Stossel, T. P. 1994 The mechanical properties of actin gels. *J. Biol. Chem.* **269**, 32 503–32 513.

Jülicher, F., Kruse, K., Prost, J. & Joanny, J.-F. 2007 Active behavior of the cytoskeleton *Phys. Rep.* **449**, 3–28. (doi:10.1016/j.physrep.2007.02.018)

Karpeev, D., Aranson, I. S., Tsimring, L. S. & Kaper, H. G. 2007 Interactions of semiflexible filaments and molecular motors. *Phys. Rev. E* **76**, 051905. (doi:10.1103/PhysRevE.76.051905)

Kasza, K. E., Rowat, A. C., Liu, J., Angelini, T. E., Brangwynne, C. P., Koederink, G. H. & Weitz, D. A. 2007 The cell as a material. *Curr. Opin. Cell Biol.* **19**, 101–107. (doi:10.1016/j.ceb.2006.12.002)

Koppen, M., Simske, J. S., Sims, P. A., Firestein, B. L., Hall, D. H., Radice, A. D., Rongo, C. & Hardin, J. D. 2001 Cooperative regulation of AJM-1 controls junctional integrity in *Caenorhabditis elegans* epithelia. *Nat. Cell Biol.* **3**, 983–991. (doi:10.1038/ncb1101-983)

Kruse, K., Joanny, J.-F., Jülicher, F., Prost, J. & Sekimoto K. 2005 Generic theory of active polar gels: a paradigm for cytoskeletal dynamics. *Eur. Phys. J. E* **16**, 5–16. (doi:10.1140/epje/e2005-00002-5)

Labouesse, M. 2006 Epithelial junctions and attachments. In *WormBook* (ed. The *C. elegans* Research Community). http://www.wormbook.org. (doi:10.1895/wormbook.1.56.1)

Li, T. 2008 A mechanics model of microtubule buckling in living cells. *J. Biomech.* **41**, 1722–1729. (doi:10.1016/j.jbiomech.2008.03.003)

Lim, C. T., Zhou, E. H. & Quek, S. T. 2006 Mechanical models for living cells—a review. *J. Biomech.* **39**, 195–216. (doi:10.1016/j.jbiomech.2004.12.008)

Lulevich, V., Zink, T., Chen, H. Y., Liu, F. T. & Liu, G. Y. 2006 Cell mechanics using atomic force microscopy-based single-cell compression. *Langmuir* **22**, 8151–8155. (doi:10.1021/la060561p)

Pampaloni, F. & Florin, E. L. 2008 Microtubule architecture: inspiration for novel carbon nanotube-based biomimetic materials. *Trends Biotechnol.* **26**, 302–310. (doi:10.1016/j.tibtech.2008.03.002)

Piekny, A. J., Johnson, J. L. F., Cham, G. D. & Mains, P. E. 2003 The *Caenorhabditis elegans* nonmuscle myosin genes *nmy-1* and *nmy-2* function as redundant components of

the *let-502*/Rho-binding kinase and *mel-11*/myosin phosphatase pathway during embryonic morphogenesis. *Development* **130**, 5695–5704. (doi:10.1242/dev.00807)

Priess, J. R. & Hirsh, D. I. 1986 *Caenorhabditis elegans* morphogenesis: the role of the cytoskeleton in elongation of the embryo. *Dev. Biol.* **117**, 156–173. (doi:10.1016/0012-1606(86)90358-1)

Purohit, P. K., Arsenault, M. E., Goldman, Y. & Bau H. H. 2008 The mechanics of short rod-like molecules in tension. *Int. J. Non-Linear Mech.* **43**, 1056–1063. (doi:10.1016/j.ijnonlinmec.2008.05.009)

Qiu, G. Y. & Pence, T. J. 1997*a* Remarks on the behavior of simple directionally reinforced incompressible nonlinearly elastic solids. *J. Elast.* **49**, 1–30. (doi:10.1023/A:1007410321319)

Qiu, G. Y. & Pence, T. J. 1997*b* Loss of ellipticity in plane deformations of a simple directionally reinforced incompressible nonlinearly elastic solid. *J. Elast.* **49**, 31–63. (doi:10.1023/A:1007441804480)

Quintin, S., Gally, C. & Labouesse, M. 2008 Epithelial morphogenesis in embryos: asymmetries, motors and brakes. *Trends Genet.* **24**, 221–230. (doi:10.1016/j.tig.2008.02.005)

Schröder, J. & Neff, P. 2003 Invariant formulation of hyperelastic transverse isotropy based on polyconvex free energy functions. *Int. J. Solids Struct.* **40**, 401–445. (doi:10.1016/S0020-7683(02)00458-4)

Shelton, C. A., Carter, J. C., Ellis, G. C. & Bowerman, B. 1999 The nonmuscle myosin regulatory light chain gene *mlc-4* is required for cytokinesis, anterior–posterior polarity, and body morphology during *Caenorhabditis elegans* embryogenesis. *J. Cell Biol.* **146**, 439–451. (doi:10.1083/jcb.146.2.439)

Shi, Y. J., Guo, W. L. & Ru, C. Q. 2008 Relevance of Timoshenko-beam model to microtubules of low shear modulus. *Physica E* **41**, 213–219 (doi:10.1016/j.physe.2008.06.025)

Spencer, A. J. M. 1984 Constitutive theory for strongly anisotropic solids. In *Continuum theory of the mechanics of fibre-reinforced composites* (ed. A. J. M. Spencer). CISM Courses and Lectures, no. 282, pp. 1–32. Wien, Austria: Springer.

Storm, C., Pastore, J. J., MacKintosh, F. C., Lubensky, T. C. & Janmey, T. A. 2005 Nonlinear elasticity in biological gels. *Nature* **435**, 191–194. (doi:10.1038/nature03521)

Taute, K. M., Pampaloni, F., Frey, E. & Florin, E.-L. 2008 Microtubule dynamics depart from wormlike chain model. *Phys. Rev. Lett.* **100**, 028102. (doi:10.1103/PhysRevLett.100.028102)

Wagner, O. I., Rammensee, S., Korde, N., Wen, Q., Letterrier, J.-F. & Janmey, P. A. 2007 Softness, strength and self-repair in intermediate filament networks. *Exp. Cell Res.* **313**, 2228–2235. (doi:10.1016/j.yexcr.2007.04.025)

Williams, B. D. & Waterston, R. H. 1994 Genes critical for muscle development and function in *Caenorhabditis elegans* identified through lethal mutations. *J. Cell Biol.* **124**, 475–490. (doi:10.1083/jcb.124.4.475)

Wissmann, A., Ingles, J. & Mains, P. E. 1997 *Caenorhabditis elegans* LET-502 is related to Rho-binding kinases and human myotonic dystrophy kinase and interacts genetically with a homolog of the regulatory subunit of smooth muscle myosin phosphatase to affect cell shape. *Genes Dev.* **11**, 409–422. (doi:10.1101/gad.11.4.409)

Woo, W. M., Goncharov, A. & Jin, Y. S. 2004 Intermediate filaments are required for *C. elegans* epidermal elongation. *Dev. Biol.* **267**, 216–229. (doi:10.1016/j.ydbio.2003.11.007)